First-principles study on doping and phase stability of HfO_2

Choong-Ki Lee,[1] Eunae Cho,[1] Hyo-Sug Lee,[2] Cheol Seong Hwang,[3] and Seungwu Han[1,*]
[1]*Department of Physics, Ewha Womans University, Seoul 120-750, Korea*
[2]*Samsung Advanced Institute of Technology, Suwon 400-600, Korea*
[3]*Department of Materials Science and Engineering and Inter-University Semiconductor Research Center, Seoul National University, Seoul 151-742, Korea*

(Received 11 March 2008; published 3 July 2008)

Based on density functional methods, relative stabilities between monoclinic, tetragonal, and cubic phases of HfO_2 with cation dopants or oxygen vacancies are investigated. It is found that dopants such as Si, Ge, Sn, P, Al or Ti with ionic radii smaller than Hf stabilize the tetragonal phase but destabilize the cubic phase. In contrast, larger dopants such as Y, Gd or Sc favor the cubic phase. The ionized oxygen vacancies compensating trivalent dopants greatly stabilize both cubic and tetragonal phases. Microscopic explanations on the results are also given. The metastable phase favored by each dopant is in good agreement with experimental data. Our results can serve as a useful guide in selecting dopants to stabilize a specific phase.

DOI: 10.1103/PhysRevB.78.012102 PACS number(s): 71.15.Nc, 74.62.Dh, 85.40.Ry

The continuous downscaling of complementary metal-oxide semiconductor (CMOS) devices with performance enhancement has been enabled by reducing the thickness of gate insulators. As the thickness of SiO_2, the traditional gate dielectric, is reduced to a few nanometers, leakage currents due to the quantum tunneling have increased greatly. The introduction of an insulator with a dielectric constant (k) higher than for SiO_2 can solve the leakage problem as it allows for increasing the physical thickness of the gate insulator. Among various oxides explored to date, hafnia (HfO_2) and its family materials are considered to be the most promising as a high-k gate oxide since they satisfy various technical requirements.

There are several polymorphs in HfO_2 such as monoclinic (m), tetragonal (t) or cubic (c) phases (see Fig. 1). The orthorhombic phase is also observed at high pressure conditions.[1] While m-HfO_2 is stable at ambient conditions, the material undergoes a phase transition to the tetragonal phase at 2000 K and to the cubic phase at 2900 K. The calculated dielectric constants vary widely from phase to phase, and the average dielectric constants are much higher for cubic and tetragonal phases.[2,3] Thin films of HfO_2 (typical thickness of $\sim$5 nm) deposited in CMOS devices are usually amorphous due to the low growth temperature ($\sim$300 °C) and they crystallize into the monoclinic phase upon annealing at temperatures above 700 °C. The two structures are similar in local bonding configurations and have dielectric constants significantly lower than those of cubic or tetragonal phases.[4] This suggests that the dielectric constant of the HfO_2 thin film can be increased without changing materials if the relative stability among polymorphs can be controlled in a way to make a high-temperature phase to be most stable at growth conditions. Recently, a series of experiments have demonstrated that such a phase control can be achieved by cation doping. For example, the doping with Si,[5] Al (Refs. 6 and 7) or Zr (Ref. 8) atoms leads to thin films with a significant portion of t-HfO_2. It was also observed that c-HfO_2 is stabilized by using Y,[9–11] Gd,[12] Sc (Ref. 13) or Dy (Ref. 13) dopants. Despite the accumulating data on the phase control of HfO_2 based on the doping method, the microscopic origin has not been elaborated much although the mechanism would be similar to the case of ZrO_2 (Ref. 14) in some parts. In addition, theoretical studies are very rare.[15]

In this Brief Report, we theoretically investigate the effect of dopants on the relative stability between m-, t- and c-HfO_2. We employ first-principles methods based on the density functional theory. For the computation of total energies and structural optimizations, we use VASP.[16] Supercells including 96 atomic sites are used for all structures. These supercells are obtained by expanding structures in Fig. 1 twice along each axis. The energy cutoff for the plane-wave basis is chosen to be 500 eV and k-points are sampled on $2\times2\times2$ uniform grids. Gaussian broadening is used with a width of 0.05 eV to smear the density of states. The exchange-correlation interactions between electrons are described by the generalized gradient approximation (GGA) (Ref. 17) and projector-augmented wave (PAW) potentials are used for the description of ion-electron interactions.[18] The atomic positions and cell parameters are relaxed until the atomic forces and stress tensors are reduced to within 0.02 eV/Å and 1 kbar, respectively. The optimized structural parameters are given in Table I, and the agreements with other work and experimental data are within 2%.

As a dopant, we choose Si, P, Ge, Al, Y, Ti, Zr, Gd, and Sc, and replace one of Hf atoms with the dopant. (All Hf sites are equivalent.) This corresponds to a doping concentration of 3.125%. In addition, we also consider oxygen vacancies since they are introduced to compensate trivalent dopants (such as Al, Y, Gd or Sc). As the vacancy site loses electrons in this case, the doubly ionized vacancy (V_O^{2+}), as well as the neutral one (V_O^0), is studied.

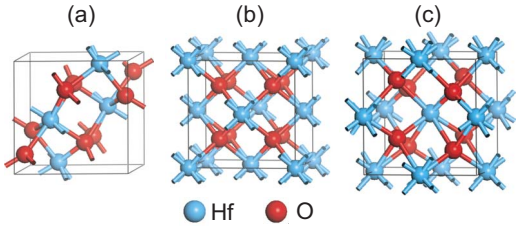

FIG. 1. (Color online) The structure of HfO_2 in (a) monoclinic, (b) cubic, and (c) tetragonal phases.

TABLE I. The structural parameters of c-, t-, and m-HfO_2. Only nontrivial parameters are shown.

Phase	This work	Other theory[a]	Experiment[b]
Monoclinic	a=5.12 Å, b=5.20 Å, c=5.28 Å, β=99.7°	a=5.22 Å, b=5.29 Å, c=5.35 Å, β=99.7°	a=5.12 Å, b=5.17 Å, c=5.30 Å, β=99.2°
Cubic	a=5.05 Å	a=5.15 Å	a=5.08 Å
Tetragonal	a=5.06 Å, c=5.20 Å	a=5.17 Å, c=5.22 Å	a=5.15 Å, c=5.29 Å

[a]Reference 1.
[b]References 19–21.

The main computational results are presented in Table II. The effective ionic radii[22] are also shown for the purpose of analysis. The relative energies ($\Delta E'$s) of t- and c-HfO_2 with respect to that of m-HfO_2 are calculated per supercell. The energies of crystalline phases without defects or dopants follow the order of $m<t<c$, in agreement with a previous calculation.[1] From Table II, one can see that there are two types of dopants. The "type-I" dopant represented by Si, Ge, Sn, P, Al, and Ti decreases ΔE_{tetra} but increases ΔE_{cubic}. In "type-II" dopants such as Y, Gd or Sc, ΔE_{cubic} is reduced further than ΔE_{tetra} although overall magnitudes of the changes are smaller than for type-I dopants. This means that type-II dopants tend to stabilize the cubic phase.

First, we explain the pronounced effect of Si doping.[15] The coordination number of the cation in t-HfO_2 is eight, the same as in c-HfO_2, and the Hf-O bond lengths are equally distributed at 2.07 and 2.37 Å. As a result of structural relaxations, four O atoms nearest to Si are pulled to the dopant site and the second-nearest O atoms relax outward [see Fig. 2(a)]. The resulting local structure is reminiscent of SiO_2 where four O atoms form a tetrahedron with the Si atom at the center. Furthermore, the relaxed Si-O bond length of 1.69 Å and O-Si-O bond angles of 105.4° or 117.9° are close to 1.63 Å and 108.9°–110.5° in the quartz structure of SiO_2, which were obtained with the same computational setup. Consequently, the local environment around the Si atom is similar to that in the quartz, explaining why the Si dopant strongly favors t-HfO_2. In c-HfO_2, eight O atoms surrounding the Si dopant relax inward symmetrically and the resulting Si-O bond length is reduced from 2.19 Å to 2.08 Å. However, this is much longer than the ideal Si-O bonding distance. To examine the possibility of a spontaneous symmetry lowering in the Si-doped c-HfO_2, we initially displace four O atoms in the tetrahedral configuration toward the dopant and perform the structural relaxation. It is found that the structure eventually transforms to m-HfO_2 indicating that c-HfO_2 becomes unstable upon Si doping. In the crystalline m-HfO_2, on the other hand, the coordination number of the cation is seven with bond lengths ranging over 2.02–2.19 Å. The relaxed structure with the Si dopant shows that five Si-O bonds are shortened by ~0.3 Å while two Si-O bonds are elongated by 0.2–0.7 Å. The reduction of the coordination number is similar to t-HfO_2, but bond lengths and angles are less ideal.

TABLE II. The relative energies of tetragonal (ΔE_{tetra}) and cubic phases (ΔE_{cubic}) with respect to that of the monoclinic phase. The energies in parentheses show the difference from the value for the perfect lattice. The ionic radii are also shown with coordination numbers indicated within parentheses. The ionic radii for the Hf atom are 0.76 and 0.83 Å for seven- and eightfold coordination, respectively.

Dopant	Ionic radius (Å)	ΔE_{tetra} (eV/supercell)	ΔE_{cubic} (eV/supercell)
Perfect		5.47	8.09
Si	0.26(4)	3.90(−1.57)	10.38(+2.29)
Ge	0.39(4)	4.55(−0.92)	9.21(+1.12)
Sn	0.55(4)	5.31(−0.16)	8.29(+0.20)
P	0.17(4)	5.00(−0.47)	10.90(+2.81)
Al	0.39(4)	5.01(−0.46)	8.77(+0.68)
Ti	0.42(4)	5.32(−0.15)	8.59(+0.50)
Y	0.96(7)	5.40(−0.07)	7.54(−0.55)
Gd	1.00(7)	5.24(−0.23)	7.38(−0.71)
Sc	0.87(8)	5.68(+0.21)	7.95(−0.14)
Zr (50%)	0.84(8)	4.74(−0.73)	6.91(−1.18)
V_O^0(fourfold site)		5.16(−0.31)	7.75(−0.34)
V_O^{2+}(threefold site)		3.30(−2.17)	4.42(−3.67)

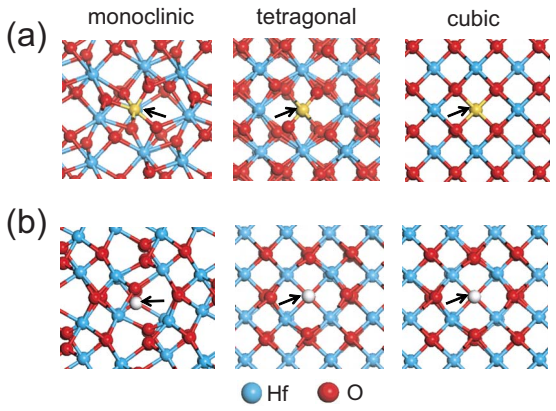

FIG. 2. (Color online) Relaxation patterns around (a) Si dopants or (b) ionized oxygen vacancies. The dopant and vacancy sites are denoted by arrows.

The above discussion also applies to other type-I dopants. As can be seen in Table II, the ionic radii of all type-I dopants are significantly smaller than those of Hf atoms (0.76–0.83 Å). Therefore, type-I dopants tend to shorten the dopant-oxygen bonds. In the tetragonal phase, four Hf-O bonds are already shorter than the others, thereby facilitating the formation of stable dopant-oxygen bonds with relatively small lattice distortions. On the other hand, the ionic radii of type-II dopants are larger than those of Hf atoms, which requires the elongation of the bonds with nearby O atoms. Compared to the cubic phase, monoclinic and tetragonal phases contain several short Hf-O bonds with a length between 2.0 and 2.1 Å. Therefore, the strain energy arising from the size mismatch should be more significant in m- and t-HfO_2 and, hence, the cubic phase is favored by the oversized type-II dopants.

TABLE III. The predicted stable phases and the minimum doping concentrations required for a metastable phase to be more stable than the monoclinic phase. The experimental data are also shown for comparison.

Dopant	Stable phase	Minimum doping concentration (%)	Experiment[a]
Si	Tetragonal	10.9	Tetragonal, 5%
Ge	Tetragonal	18.6	N/A
Al	Tetragonal	11.1	Tetragonal
Y	Cubic	10.6	Cubic, 4%–6.5%
Sc	Cubic	12.8	Cubic, 10%
Gd	Cubic	9.9	Cubic, 10%–15%

[a]References 5–7 and 9–13.

Next, we discuss the effects of oxygen vacancies. It is well established that Y atoms in ZrO_2 introduce oxygen vacancies to compensate their charge states.[14] A similar process would occur in HfO_2: Being trivalent, two Y atoms substituting Hf sites results in a deficiency of two electrons, and this is compensated by the introduction of an oxygen vacancy. In m-HfO_2, there are two types of oxygen, threefold or fourfold, while all oxygen atoms are equivalent in t- and c-HfO_2. It is known that the neutral oxygen vacancy in m-HfO_2 is more stable at the fourfold site than at the threefold one, and vice versa for the charged vacancy.[23] As shown in Table II, the neutral oxygen vacancy (V_O^0) only slightly affects the relative stability. However, when the vacancy is doubly ionized, ΔE_{tetra} and ΔE_{cubic} are significantly reduced. This can be explained in terms of the coordination number of Hf atoms; Hf atoms favor a sevenfold coordination as in m-HfO_2. The charged oxygen vacancy in t- and c-HfO_2 leads to the sevenfold coordination of Hf atoms around the defect site, and this is the primary reason for the stabilization of these phases. (When the vacancy is neutral, the coordination number is effectively unchanged because defect states are occupied.) In addition to this, we note that the structural relaxation plays a role. As shown in Fig. 2(b), large atomic relaxations are noticeable around charged vacancies compared to neutral ones (not shown). Due to the effectively positive charge (+2) centered at the vacancy site, the anions relax toward the vacancy, while cations are repelled. This essentially accounts for the dielectric screening of charged defects by the lattice. From the inspection of the bonding distribution, it is found that the inward motion of oxygen atoms is noticeably suppressed in m-HfO_2, which is attributed to relatively longer O-O bonding distances in this phase. As a consequence, t- and c-HfO_2 are further stabilized by the charged vacancy, contributing to the reduction of ΔE_{tetra} and ΔE_{cubic}.

Like HfO_2, zirconia (ZrO_2) has three metastable phases of t-, c-, and m-ZrO_2. In our calculations, the doping with one Zr atom in each supercell did not give rise to noticeable changes in the relative stability. When Zr atoms randomly replace 50% of Hf atoms, however, ΔE_{tetra} and ΔE_{cubic} change considerably (see Table II). This is closely related to the phase stability among ZrO_2 polymorphs. Since the total energies of t- and c-ZrO_2 relative to m-ZrO_2 are calculated to

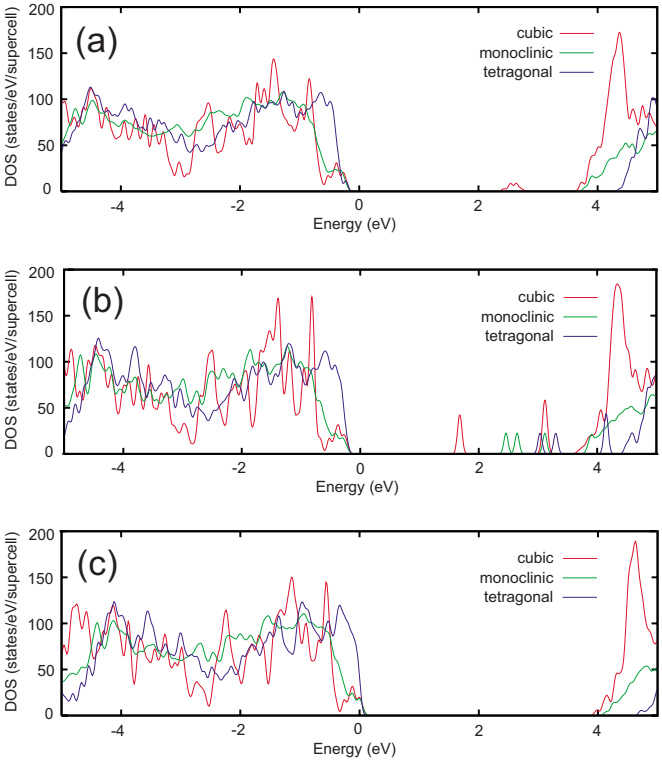

FIG. 3. (Color online) The DOS of c-, t-, and m-HfO_2 in the presence of (a) Si, (b) Ti, and (c) Y dopants. The Fermi level is set to zero.

be 4.02 eV and 5.90 eV, respectively, the alloying with Zr atoms lowers ΔE_{tetra} and ΔE_{cubic} compared to pure HfO_2. In fact, by exploring $Hf_{1-x}Zr_xO_2$ sold solutions over a wide range of x, it is found that the following linear relation holds to a good precision:

$$\Delta E(Hf_{1-x}Zr_xO_2) = (1-x)\Delta E(HfO_2) + x\Delta E(ZrO_2). \quad (1)$$

This implies that the Zr doping does not change the order of relative stability at any doping concentration. In polycrystalline thin films, the surface energy may help stabilize the tetragonal phase.[8,24]

Based on the above results, we theoretically guess which metastable phase becomes more stable than the monoclinic phase at a certain minimum doping concentration. As a first approximation, we neglect any interaction between defects and/or dopants, and ΔE at an arbitrary concentration is estimated by a linear extrapolation of the results in Table II. (However, the undersized dopants can attract the oxygen vacancy.[14]) It is also assumed that charged defects are completely compensated by oxygen vacancies. For instance, if there are two Y dopants and one oxygen vacancy within the supercell, the doping concentration corresponds to 6.25% and $\Delta E_{\text{cubic}}(2Y + V_O^{2+}) = 8.09 - 2 \times 0.55 - 3.67 = 3.32$ eV. This assumption is tested by actually introducing the defect set into the supercell. The computed ΔE_{cubic} is 3.70 eV which agrees reasonably with the simple estimation above. The results for selected dopants are given in Table III and they are also compared with experimental data when available. It is found that the estimations based on the first-principles results

agree well with the experiments. However, the minimum doping concentrations are larger than the experimental values in many cases. This might be related to the defect-dopant interactions, which need further investigations.

For type-II dopants of Y, Sc, and Gd, one can also define minimum doping concentrations, n_{c1} and n_{c2}, at which the cubic phase becomes more stable than the tetragonal phase ($\Delta E_{\text{tetra}}=\Delta E_{\text{cubic}}$), and the tetragonal phase becomes lower in energy than the monoclinic phase ($\Delta E_{\text{tetra}}=0$), respectively. The values of $n_{c1}(n_{c2})$ are 6.7(14.8), 7.4(19.5), and 6.7(13.0)% for Y, Sc, and Gd, respectively. In the case of Al doping, the cubic phase becomes more stable than the monoclinic phase at a doping concentration of 21.9% but is always unstable against the tetragonal phase. For Si- and Ge-doped HfO_2, the cubic phase is the highest in energy at any concentration of the dopant.

In Fig. 3, the density of states (DOS) is presented for the representative cases of Si, Ti and Y dopants. For the Si dopant in Fig. 3(a), gap states are found only in c-HfO_2. The inspection of the wave functions indicates that they are localized around the Si atom with s-like symmetry. The corresponding state does not exist for t- and m-HfO_2. Therefore, Si dopants in t-HfO_2 would not degrade much of leakage behaviors since they do not create trap sites. In the case of Ti doping in Fig. 3(b), gap states appear in all phases. These levels are derived from Ti-d orbitals with degeneracy lifted by the crystal field. For instance, the Ti d-levels in c-HfO_2 are split into e_g and t_{2g} states (with e_g states lower in energy) due to the crystal field with cubic symmetry. On the other hand, the Y dopant does not introduce any gap state [see Fig. 3(c)]. This is understandable because the valence electrons of the Y atom are close in energy to those of the Hf atom as is evidenced in similar energy gaps of Y_2O_3 and HfO_2. From the study on DOS's for other dopants, we find that DOS's for trivalent dopants such as Al, Gd or Sc are similar to that of Y; there is no ingap state associated with the dopant and the Fermi level lies below the valence edge. It is also observed that DOS's for tetrahedrally bonded dopants such as Ge, Sn or P in c-HfO_2 show defect levels within the energy gap, which is similar to the case of Si. The defect levels are unoccupied for Ge and Sn while they are singly occupied for P.

In summary, we investigated the energetics of HfO_2 polymorphs in the presence of various dopants and oxygen vacancies. The tetragonal phase was favored by the type-I dopants (Si, Ge, Sn, Ti, P, and Al) because ionic radii are smaller than for Hf atoms and the formation of short bonds are facilitated in t-HfO_2. On the other hand, the type-II dopants (Y, Sc, and Gd) with atomic radii larger than that of the Hf atom prefer c-HfO_2. It was also found that the ionized oxygen vacancy plays a crucial role in the stabilization of metastable phases. The stable phases estimated by the first-principles results were in good agreement with recent experimental data. Our results can serve as a useful guide in selecting dopants to stabilize a specific phase.

This work was supported by the System IC2010 program and the National Program for 0.1 Terabit NVM Devices. The computations were carried out at KISTI (Grant No. KSC-2007-S00-1006).

*Corresponding author; hansw@ewha.ac.kr

[1] J. Kang, E.-C. Lee, and K. J. Chang, Phys. Rev. B **68**, 054106 (2003).
[2] X. Zhao and D. Vanderbilt, Phys. Rev. B **65**, 233106 (2002).
[3] G.-M. Rignanese, X. Gonze, G. Jun, K. Cho, and A. Pasquarello, Phys. Rev. B **69**, 184301 (2004).
[4] X. Zhao, D. Ceresoli, and D. Vanderbilt, Phys. Rev. B **71**, 085107 (2005).
[5] K. Tomida, K. Kita, and A. Toriumi, Appl. Phys. Lett. **89**, 142902 (2006).
[6] P. K. Park and S.-W. Kang, Appl. Phys. Lett. **89**, 192905 (2006).
[7] Y. Yang, W. J. Zhu, T. P. Ma, and S. Stemmer, J. Appl. Phys. **95**, 3772 (2004).
[8] D. H. Triyoso, R. I. Hedge, J. K. Schaeffer, D. Roan, P. J. Tobin, S. B. Samavedam, B. E. White, Jr., R. Gregory, and X.-D. Wang, Appl. Phys. Lett. **88**, 222901 (2006).
[9] S.-G. Lim, S. Kriventsov, T. N. Jackson, J. H. Haeni, D. G. Schlom, A. M. Balbashov, R. Uecker, P. Reiche, J. L. Feeouf, and G. Lucovsky, J. Appl. Phys. **91**, 4500 (2002).
[10] K. Kita, K. Kyuno, and A. Toriumi, Appl. Phys. Lett. **86**, 102906 (2005).
[11] E. Rauwel, C. Dubourdieu, B. Holländer, N. Rochat, F. Ducroquet, M. D. Rossell, G. Van Tendeloo, and B. Pelissier, Appl. Phys. Lett. **89**, 012902 (2006).
[12] Y. B. Losovyj, I. Ketsman, A. Sokolov, K. D. Belashchnko, P. A. Dowben, J. Tang, and Z. Wang, Appl. Phys. Lett. **91**, 132908 (2007).
[13] C. Adelmann, V. Sriramkumar, V. Van Elshocht, P. Lehnen, T. Conard, and S. De Gendt, Appl. Phys. Lett. **91**, 162902 (2007).
[14] P. Li, I.-W. Chen, and J. E. Penner-Hahn, J. Am. Ceram. Soc. **77**, 118 (1994).
[15] D. Fischer and A. Kersch, Appl. Phys. Lett. **92**, 012908 (2008).
[16] G. Kresse and J. Hafner, Phys. Rev. B **47**, 558(R) (1993); **49**, 14251 (1994).
[17] J. P. Perdew, K. Burke, and M. Ernzerhof, Phys. Rev. Lett. **77**, 3865 (1996).
[18] P. E. Blöchl, Phys. Rev. B **50**, 17953 (1994).
[19] J. Wang, H. P. Li, and R. Stevens, J. Mater. Sci. **27**, 5397 (1992).
[20] D. M. Adams, S. Leonard, D. R. Russel, and R. J. Cemik, J. Phys. Chem. Solids **52**, 1181 (1991).
[21] D. W. Stacy, J. K. Johnstone, and D. R. Wilder, J. Am. Ceram. Soc. **55**, 482 (1972).
[22] R. D. Shannon and C. T. Prewitt, Acta Crystallogr., Sect. B: Struct. Crystallogr. Cryst. Chem. **25**, 925 (1969).
[23] A. S. Foster, F. Lopez Gejo, A. L. Shluger, and R. M. Nieminen, Phys. Rev. B **65**, 174117 (2002).
[24] S. K. Kim and C. S. Hwang, Electrochem. Solid-State Lett. **11**, G9 (2008).